

Multipole response of doped ^3He drops

Francesca Garcias, Llorenç Serra, and Montserrat Casas

Departament de Física, Universitat de les Illes Balears, E-07071 Palma de Mallorca, Spain

Manuel Barranco

Departament ECM, Facultat de Física, Universitat de Barcelona, E-08028 Barcelona, Spain

(October 26, 2018)

The multipole response of $^3\text{He}_N$ drops doped with very attractive impurities, such as a Xe atom or an SF_6 molecule, has been investigated in the framework of the Finite Range Density Functional Theory and the Random Phase Approximation. We show that volume ($L = 0$) and surface ($L = 1, 2$) modes become more fragmented, as compared with the results obtained for pure $^3\text{He}_N$ drops. In addition, the dipole mean energy goes smoothly to zero when N increases, indicating that for large N values these impurities are delocalized in the bulk of the drop.

PACS: 71.15.Mb, 67.55.Lf, 67.55.Jd

I. INTRODUCTION

The study of helium drops has been the object of extensive experimental and theoretical investigations^{1–4}. One of the goals of these studies is to understand how various bulk physical properties of the quantum liquid are modified in restricted geometries. Special mention deserves the emerging field of infrared spectroscopy of molecules inside or attached to helium droplets^{3–6} which has motivated a great theoretical activity to determine how the molecular moments of inertia are affected by the helium environment^{7,8}.

The main experimental effort has focused on the study of pure and doped $^4\text{He}_N$ drops, for which a microscopic description of the ground state (gs) using Monte Carlo techniques^{3,9–15}, and of the elementary excitations using an optimized variational method^{16,17} are available. Density functional calculations of the gs and excitation spectrum using finite-range (FRDF) or zero-range density functionals have been carried out, see Refs. 18–22 and references therein. Recently, the physical appearance of quantized vortices pinned by dopant molecules in ^4He droplets has been studied within the FRDF theory²³.

In the case of ^3He drops, experimental data are becoming available²⁴. Small ^3He drops are difficult to produce since a minimum number of atoms is needed to produce a selfbound drop²⁵, and are as difficult to observe as ^4He drops because they are neutral. Nevertheless, ^3He systems constitute the only Fermi systems capable of being observed in bulk liquid and droplets, and for this reason they have attracted some theoretical interest. Yet, microscopic calculations of ^3He droplets are scarce, and only concern the gs structure^{25–27}. A mass-formula for ^3He drops based on an extended Thomas-Fermi method has been proposed²⁸, and the binding energy of open-shell ^3He drops has been determined by a semiempirical shell-correction method²⁹. The gs of small polarized $\text{Li-}^3\text{He}_N$ clusters has been determined using the Path Integral Monte Carlo Method³⁰. Ground state properties of ^3He drops doped with some inert atoms and molecular impurities have been recently studied³¹ within the FRDF theory, as well as the gs structure of pure or doped mixed $^3\text{He-}^4\text{He}$ droplets^{32,33}. Studies of mixed droplets are relevant in connection with the experimental results presented in Ref. 5. Indeed, it is crucial to know the composition of the first solvation shells around the impurity to determine if the dopant molecule is in a superfluid environment⁵, or to determine whether the molecule may couple to bosonic or fermionic-type liquid excitations which in turn determines the dissipative picture of the molecule rotational spectrum³⁴.

Previously quoted references indicate that there has been an enormous impetus in the development and application of microscopic techniques to the description of liquid helium drops. However, current experiments sometimes have to deal with situations that cannot be addressed by fully microscopic methods. We can mention, for example, the description of very large ^4He and ^3He drops^{35,36}, or the structure of large mixed drops already discussed. As a matter of fact, in spite of the recent progress made in the variational description²⁶ of small (up to 40 atoms) ^3He droplets, a simultaneous description of ground state and elementary excitations of pure ^3He droplets has been only obtained within the density functional theory, using either zero-range^{37,38} or finite-range density functionals^{39–42}. In these situations, density functional theory results provide a useful guide to the appearance of interesting physical phenomena obtained at the price of introducing some phenomenology.

The aim of this work is to analyze the distortions caused by the presence of an impurity like a Xe atom or an SF_6 molecule in the excitation spectrum of a ^3He droplet. The solvation energies of these impurities have been found to

be negative³¹, and this makes plausible the scenario underlying in our calculation. We have analyzed this effect in the framework of the FRDF theory and the Random Phase Approximation (RPA). This paper is organized as follows: In Section II we briefly introduce the finite-range density functional we use, and the particle-hole (ph) interaction employed in the RPA calculations. In Section III we present results for the volume $L = 0$ and the low-multipolarity surface excitations. A preliminary account of the dipole response has been previously reported⁴³. In Section IV we draw the conclusions, and in an Appendix we present an example of how the angular decomposition of the ph matrix elements has been carried out.

II. THE FINITE RANGE DENSITY FUNCTIONAL AND PARTICLE-HOLE INTERACTION

In the framework of the density functional theory, the ground state of $^3\text{He}_N$ doped drops is found by minimizing the energy E written as

$$E[\rho, \tau] = \int d\vec{r} \mathcal{E}(\rho, \tau) , \quad (1)$$

where³¹

$$\begin{aligned} \mathcal{E}(\rho, \tau) = & \frac{\hbar^2}{2m^*(\vec{r})} \left[\tau(\vec{r}) - \frac{\vec{j}^2(\vec{r})}{\rho(\vec{r})} \right] \\ & + \frac{1}{2} \rho(\vec{r}) \int d\vec{r}' V_{LJ}(|\vec{r} - \vec{r}'|) \rho(\vec{r}') + \frac{c}{2} \rho^2(\vec{r}) [\bar{\rho}(\vec{r})]^\gamma + \rho(\vec{r}) V_{imp}(\vec{r}) . \end{aligned} \quad (2)$$

The particle $\rho(\vec{r})$, current $\vec{j}(\vec{r})$ and kinetic energy $\tau(\vec{r})$ densities are written in terms of the single particle (sp) wave functions $\phi_k(\vec{r})$ obtained solving the Kohn-Sham (KS) equations deduced from Eq. (2). For systems having an effective mass $m^*(r)$, the inclusion of a term \vec{j}^2/ρ in Eq. (2) guarantees that the density functional is Galilean invariant⁴⁴. This term has no influence on the ground state of time-reversal invariant, spin-saturated droplets, and for this reason it is usually omitted. However, its contribution to the ph interaction for systems like the present one, in which the impurity is treated as an external field breaking the translational invariance of the system, cannot be neglected.

In the above expression $V_{LJ}(|\vec{r} - \vec{r}'|)$ is the Lennard-Jones interatomic potential screened at short distances

$$V_{LJ}(r) = \begin{cases} 4\epsilon \left[(\sigma/r)^{12} - (\sigma/r)^6 \right] & \text{if } r \geq \sigma \\ b_{LJ} \left[1 - (r/\sigma)^8 \right] & \text{otherwise ,} \end{cases} \quad (3)$$

and the averaged density $\bar{\rho}(\vec{r})$ is defined as

$$\bar{\rho}(\vec{r}) = \int d\vec{r}' \rho(\vec{r}') W(|\vec{r} - \vec{r}'|) \quad (4)$$

with

$$W(r) = \begin{cases} 3/(4\pi\sigma^3) & \text{if } r < \sigma \\ 0 & \text{otherwise .} \end{cases} \quad (5)$$

The effective mass m^* is parametrized as $m^* = m(1 - \bar{\rho}/\rho_c)^{-2}$. The set of coefficients entering the definition of $\mathcal{E}(\rho, \tau)$ can be found in Table I of Ref. 31. V_{imp} is the helium-impurity potential taken from Ref. 45 in the case of Xe, and from Ref. 46 in the case of SF₆, in its spherically averaged version. In both cases we have assumed that the impurity is an object of infinite mass located at the coordinate origin.

The distortion of the ground state structure of ^3He drops due to the presence of impurities has been described in detail in Ref. 31. To analyze the multipole excitations induced by an external field that couples to the particle density of the drop, we have used the time-dependent version of the density functional theory. For sufficiently weak external fields the response can be treated linearly within the RPA. In this approximation the elementary excitations of the system are described in terms of correlated ph transitions. The amplitude of a particular excited state in the basis of a discrete space of ph transitions is obtained by diagonalizing the Hamiltonian $H = H_0 + V_{ph}$, which is the sum of the KS Hamiltonian H_0 plus the ph interaction V_{ph} . This is done solving the RPA equation^{47,48}

$$\begin{pmatrix} A & B \\ -B^* & -A^* \end{pmatrix} \begin{pmatrix} X^{(\lambda)} \\ Y^{(\lambda)} \end{pmatrix} = \omega_\lambda \begin{pmatrix} X^{(\lambda)} \\ Y^{(\lambda)} \end{pmatrix}, \quad (6)$$

where the matrices A and B are written in terms of matrix elements of the interaction between the ph pairs that can be coupled to have the desired angular momentum.

Writing the particle, current and kinetic energy densities in terms of the sp basis $\phi_k(\vec{r})$ and the occupation numbers p_{kl}

$$\rho(\vec{r}) = \sum_{kl} \phi_k^*(\vec{r}) p_{kl} \phi_l(\vec{r}) \quad (7)$$

$$\vec{j}(\vec{r}) = \frac{1}{2i} \sum_{kl} (\vec{\nabla} - \vec{\nabla}') \phi_k^*(\vec{r}') p_{kl} \phi_l(\vec{r}) |_{\vec{r}=\vec{r}'} \quad (8)$$

$$\tau(\vec{r}) = \sum_{kl} \vec{\nabla} \vec{\nabla}' \phi_k^*(\vec{r}) p_{kl} \phi_l(\vec{r}') |_{\vec{r}=\vec{r}'} , \quad (9)$$

the ph interaction is obtained^{47,49} from the second variation of the energy functional with respect to the occupation numbers:

$$V_{ijkl} \equiv \langle ij | V_{ph}(\vec{r}_1, \vec{r}_2) | kl \rangle = \frac{\delta^2 E}{\delta p_{ik} \delta p_{jl}}. \quad (10)$$

If $m^* = m$ in the density functional (a situation which we indicate with the notation $E = E[\rho]$), the second variation of the energy with respect to the occupation numbers taken at the ground state straightforwardly provides the ph interaction V_{ph} . This variation can be obtained as

$$\begin{aligned} \frac{\delta^2 E[\rho]}{\delta p_{ik} \delta p_{jl}} &= \int d\vec{r}_1 d\vec{r}_2 \left(\frac{\delta^2 E[\rho]}{\delta \rho(\vec{r}_2) \delta \rho(\vec{r}_1)} \right)_{gs} \frac{\delta \rho(\vec{r}_1)}{\delta p_{ik}} \frac{\delta \rho(\vec{r}_2)}{\delta p_{jl}} \\ &= \int d\vec{r}_1 d\vec{r}_2 \phi_i^*(\vec{r}_1) \phi_j^*(\vec{r}_2) \left(\frac{\delta^2 E[\rho]}{\delta \rho(\vec{r}_2) \delta \rho(\vec{r}_1)} \right)_{gs} \phi_k(\vec{r}_1) \phi_l(\vec{r}_2), \end{aligned} \quad (11)$$

and comparing with Eq. (10) it results

$$V_{ph}(\vec{r}_1, \vec{r}_2) = \left(\frac{\delta^2 E[\rho]}{\delta \rho(\vec{r}_2) \delta \rho(\vec{r}_1)} \right)_{gs}. \quad (12)$$

The presence of a position-dependent effective mass in the functional introduces a velocity dependence in the ph interaction. In this case Eq. (10) becomes

$$\begin{aligned} V_{ijkl} &= \int d\vec{r}_1 d\vec{r}_2 \left(\frac{\delta^2 E}{\delta \rho(\vec{r}_1) \delta \rho(\vec{r}_2)} \frac{\delta \rho(\vec{r}_1)}{\delta p_{ik}} \frac{\delta \rho(\vec{r}_2)}{\delta p_{jl}} \right. \\ &\quad + \frac{\delta^2 E}{\delta \rho(\vec{r}_1) \delta \tau(\vec{r}_2)} \frac{\delta \rho(\vec{r}_1)}{\delta p_{ik}} \frac{\delta \tau(\vec{r}_2)}{\delta p_{jl}} \\ &\quad + \frac{\delta^2 E}{\delta \tau(\vec{r}_1) \delta \rho(\vec{r}_2)} \frac{\delta \tau(\vec{r}_1)}{\delta p_{ik}} \frac{\delta \rho(\vec{r}_2)}{\delta p_{jl}} \\ &\quad + \frac{\delta^2 E}{\delta \tau(\vec{r}_1) \delta \tau(\vec{r}_2)} \frac{\delta \tau(\vec{r}_1)}{\delta p_{ik}} \frac{\delta \tau(\vec{r}_2)}{\delta p_{jl}} \\ &\quad \left. + \frac{\delta^2 E}{\delta j^{(\alpha)}(\vec{r}_1) \delta j^{(\alpha)}(\vec{r}_2)} \frac{\delta j^{(\alpha)}(\vec{r}_1)}{\delta p_{ik}} \frac{\delta j^{(\alpha)}(\vec{r}_2)}{\delta p_{jl}} \right) \end{aligned} \quad (13)$$

with

$$\begin{aligned}\frac{\delta\tau(\vec{r})}{\delta p_{kl}} &= \vec{\nabla} \phi_k^*(\vec{r}) \vec{\nabla} \phi_l(\vec{r}) , \\ \frac{\delta j^{(\alpha)}(\vec{r}_1)}{\delta p_{kl}} &= \frac{1}{2i} \left[\phi_k^*(\vec{r}_1) (\vec{\nabla}_1 - \overleftarrow{\nabla}_1) \phi_l(\vec{r}_2) \right]_{\vec{r}_1=\vec{r}_2} .\end{aligned}\quad (14)$$

The arrow on the gradient operators indicates whether they act on the left or on the right. The terms arising from current derivatives are essential to fulfill the Thomas-Reiche-Kuhn (or energy-weighted) sum rule. The contribution of current terms to the ph interaction is

$$\begin{aligned}V_{ijkl} &= \int d\vec{r}_1 d\vec{r}_2 \left(\frac{\delta^2 E}{\delta j^{(\alpha)}(\vec{r}_1) \delta j^{(\alpha)}(\vec{r}_2)} \right) \frac{\delta j^{(\alpha)}(\vec{r}_1)}{\delta p_{ik}} \frac{\delta j^{(\alpha)}(\vec{r}_2)}{\delta p_{jl}} \\ &= \frac{-\hbar^2}{4m} \int d\vec{r}_1 d\vec{r}_2 \phi_i^*(\vec{r}_1) \phi_j^*(\vec{r}_2) (\vec{\nabla}_1 - \overleftarrow{\nabla}_1) \left(\frac{\delta^2 E}{\delta j^{(\alpha)}(\vec{r}_1) \delta j^{(\alpha)}(\vec{r}_2)} \right) (\vec{\nabla}_2 - \overleftarrow{\nabla}_2) \phi_k(\vec{r}_1) \phi_l(\vec{r}_2) ,\end{aligned}\quad (15)$$

where a sum over the three components α is assumed, and the gradients only act on the sp wave functions. This expression coincides with the back-flow contribution to the ph interaction for ^4He drops²¹.

Particularizing to the density functional Eq. (2), accounting for Eqs. (14), (15) and that $\frac{\delta^2 E}{\delta\tau(\vec{r}_1)\delta\tau(\vec{r}_2)} = 0$, Eq. (13) gives for the ph interaction

$$\begin{aligned}V_{ph}(\vec{r}_1, \vec{r}_2) &= V_{LJ}(|\vec{r}_1 - \vec{r}_2|) + c [\bar{\rho}(\vec{r}_1)]^\gamma \delta(\vec{r}_1 - \vec{r}_2) \\ &\quad + c \gamma \left\{ \rho(\vec{r}_1) [\bar{\rho}(\vec{r}_1)]^{(\gamma-1)} + \rho(\vec{r}_2) [\bar{\rho}(\vec{r}_2)]^{(\gamma-1)} \right\} W(|\vec{r}_1 - \vec{r}_2|) \\ &\quad + \frac{1}{2} \gamma (\gamma - 1) c \int d\vec{r} \rho^2(\vec{r}) [\bar{\rho}(\vec{r})]^{(\gamma-2)} W(|\vec{r}_1 - \vec{r}|) W(|\vec{r}_2 - \vec{r}|) \\ &\quad + \int d\vec{r} \frac{\hbar^2}{2m} \frac{2}{\rho_c^2} \tau(\vec{r}) W(|\vec{r}_1 - \vec{r}|) W(|\vec{r}_2 - \vec{r}|) \\ &\quad + \overleftarrow{\nabla}_1 f(\vec{r}_1) W(|\vec{r}_1 - \vec{r}_2|) \vec{\nabla}_1 + \overleftarrow{\nabla}_2 f(\vec{r}_2) W(|\vec{r}_1 - \vec{r}_2|) \vec{\nabla}_2 \\ &\quad + g(\vec{r}_1) \delta(\vec{r}_1 - \vec{r}_2) (\vec{\nabla}_1 - \overleftarrow{\nabla}_1) (\vec{\nabla}_2 - \overleftarrow{\nabla}_2)\end{aligned}\quad (16)$$

with

$$f(\vec{r}_i) = \frac{\hbar^2}{2m} \left(\frac{2}{\rho_c^2} \bar{\rho}(\vec{r}_i) - \frac{2}{\rho_c} \right) \quad (17)$$

and

$$g(\vec{r}) = \frac{\hbar^2}{4m} \left[\left(\frac{\bar{\rho}(\vec{r})}{\rho_c} \right)^2 - 2 \frac{\bar{\rho}(\vec{r})}{\rho_c} \right] \frac{1}{\rho(\vec{r})} . \quad (18)$$

Equation (16) shows that in addition to the Lennard-Jones potential V_{LJ} , Eq. (3), the ph interaction has finite-range terms, velocity dependent components, and other terms which combine both finite-range and velocity dependence through the presence of gradient operators.

The next task is to calculate the matrix elements in the ph basis. This is greatly simplified in the case of droplets with a magic number of ^3He atoms, the only droplets studied here. In this case, the mean field is spherically symmetric and the angular part of the sp wave functions is a spherical harmonic. Performing a multipole expansion of the ph interaction, the sum over third components can be done and only radial integrals remain to be numerically computed (see the Appendix for details). This allows one to compute the RPA matrices A and B . After diagonalizing Eq. (6), the strength function from the gs $|0\rangle$ to the set of excited states $\{|n\rangle\}$ (with excitation energies $\{\omega_n\}$) is obtained as

$$S(\omega) = \sum_n \delta(\omega - \omega_n) |\langle n|Q_L|0\rangle|^2 , \quad (19)$$

where Q_L is the excitation operator for which we have made the natural choices $Q_0 = \sum_i r_i^2$ for $L = 0$ (volume mode), and $Q_L = \sum_i r_i^L Y_{L0}(\Omega_i)$ for $L = 1, 2$ (surface modes).

The transition matrix element of the strength function is obtained in terms of the solutions of RPA equation and the sp radial wave functions u_i defined in the Appendix. The explicit expression for surface modes is given by

$$\langle 0|Q_L|n\rangle = \frac{1}{\sqrt{2L+1}} \sum_{mi} (X_{mi}^{(n)} - Y_{mi}^{(n)}) \langle u_m|r^L|u_i\rangle \langle \ell_m||Y_L||\ell_i\rangle, \quad (20)$$

where $\langle \ell_m||Y_L||\ell_i\rangle$ is the angular reduced matrix element of the excitation operator⁵⁰. The corresponding expression for the monopole mode is

$$\langle 0|Q_0|n\rangle = \sum_{mi} (X_{mi}^{(n)} - Y_{mi}^{(n)}) \langle u_m|r^2|u_i\rangle \delta_{\ell_m\ell_i}. \quad (21)$$

The transition (also called induced) densities for the operator $Q_L = \sum_i r_i^L Y_{L0}(\Omega_i)$ that causes surface excitations are obtained as

$$\rho_{n0}(r) = \frac{1}{\sqrt{2L+1}} \sum_{mi} (X_{mi}^{(n)} - Y_{mi}^{(n)}) \langle \ell_m||Y_L||\ell_i\rangle \frac{u_m(r)u_i(r)}{r^2}, \quad (22)$$

and $\langle 0|Q_L|n\rangle = \int dr r^{2+L} \rho_{n0}(r)$. The corresponding induced densities for the monopole mode are given by

$$\rho_{n0}(r) = \sum_{mi} (X_{mi}^{(n)} - Y_{mi}^{(n)}) \frac{u_m(r)u_i(r)}{r^2} \delta_{\ell_m\ell_i}, \quad (23)$$

and $\langle 0|Q_0|n\rangle = \int dr r^4 \rho_{n0}(r)$.

Obviously, the dimension of matrices A and B depends on how many particle-hole pairs mi are taken after discretizing the continuum. We have included enough sp states so that the Thomas-Reiche-Kuhn sum rule is satisfied within 98%. We have also checked that for pure drops the dipole mode is at zero energy due to the translational invariance of the system.

To finish this Section, we would like to recall that originally, density functionals for liquid ^3He were obtained from a contact, velocity-dependent ^3He - ^3He effective interaction⁵¹ that made it rather simple to evaluate the contribution of direct *and* exchange terms to the total energy and to the ph interaction. Later on, a finite-range component was added to the contact interaction to improve its properties at finite momentum. This is the origin of the screened Lennard-Jones potential^{52,53}, which takes care of two major characteristics of the interatomic potential the original effective He-He interaction lacked, namely the hard core repulsion at short distances, and the asymptotic r^{-6} behavior. Thus, exchange effects, which are known to be large in liquid ^3He , are phenomenologically accounted for in the density functional through the effective parameters entering its definition.

III. RESULTS

A. Monopole mode

Figure 1 shows a comparison between the monopole ('breathing mode') spectrum of pure and doped drops. It is seen that the presence of the impurity increases the fragmentation of the spectra in the high energy region. This effect is more important for small clusters and more attractive impurities. In both cases of pure and doped drops, the mean energy defined as $\bar{\omega} = \sum_j \omega_j S(\omega_j) / \sum_j S(\omega_j)$ lies above the atom emission threshold (Fermi energy changed of sign) and decreases as the number of ^3He atoms of the drop increases (see Figs. 2 and 3). It is worthwhile to recall that for pure $^4\text{He}_N$ droplets, except for rather small N values the monopole strength is in the discrete region of the spectrum^{16,18,20}, and that the presence of a Xe or SF_6 impurity also increases the fragmentation of the spectrum; for small drops the monopole strength lies in the continuum region^{20,22}.

We display in Fig. 4 the transition densities corresponding to the more intense monopole peaks of $\text{Xe}+^3\text{He}_{40}$. This figure shows the well-known fact that the monopole is a volume mode: the induced densities have a node and penetrate inside the drop. The bulk oscillations are connected with the oscillations in the drop density $\rho(r)$, also shown in Fig. 4, which are due to the distribution of ^3He atoms in solvation shells around the dopant on the one hand, and to the repulsive core of the effective interaction, on the other hand.

B. Dipole mode

The $L = 1$ spectrum shows again that fragmentation increases for the more attractive impurities (see Fig. 5). In this case the mean dipole energy always lies below the continuum threshold and decreases with the number of ^3He

atoms of the drop. In spite that small doped drops are stable to dipole fluctuations since a large energy is needed to induce the oscillation of the impurity against the ^3He atoms, Fig. 3 shows that when the drop size increases the dipole mean energy rapidly decreases and the mode eventually becomes unstable. This is considered a clear signature that the impurity is delocalized in the bulk of the drop^{17,22,43}. The dipole mode has also been found to be unstable²² for large $^4\text{He}_N$ drops doped with inert atoms and SF_6 , for which the mean dipole energy lies in the discrete part of the spectrum.

C. Quadrupole mode

Fig. 6 shows that, as compared to the pure case, the presence of a rather attractive impurity pushes this mode downwards in energy. When this causes the quadrupole mode to move from the continuum to the discrete part of the energy spectrum, the fragmentation decreases and the peak becomes more collective. This is the case for $N = 40$, for example. For larger drops, the quadrupole mode is below the atom emission threshold, see Fig. 3 (this also happens in pure drops), and the effect is not so clearly seen.

Examples of induced densities for dipole and quadrupole modes are shown in Fig. 7. They are localized at the drop surface, as it corresponds to the surface character of these modes.

We would like to close this Section indicating that in the case of pure ^3He droplets, a comparison with results for $L = 0$ and 2 modes obtained using density functionals built using fairly different strategies^{38,39} yields an overall good agreement.

IV. CONCLUSIONS

We have investigated the multipole collective excitations of $^3\text{He}_N$ drops doped with Xe atoms and SF_6 molecules in the framework of the FRDF theory plus the RPA. A comparison with the results for pure drops shows that the presence of these strongly attractive impurities increases the spectrum fragmentation. This effect appears in volume and surface modes as well, and it is more marked for small clusters and more attractive impurities.

The presence of an attractive impurity decreases the mean energy of surface modes as in the case of doped $^4\text{He}_N$ clusters²². For large clusters the mean energy of surface modes lies below the atom emission threshold, whereas for the monopole volume mode it is always above the threshold.

When the cluster size increases the dipole mean excitation goes to zero, indicating that the impurity is delocalized in the bulk of the drop for ^3He clusters doped with Xe and SF_6 impurities. A similar effect was found in ^4He clusters. From the experience gathered in the case of ^4He clusters, we may conclude that whereas the precise value of the (rather fragmented) collective modes may be sensitive to the arbitrariness introduced in the choice of some of the FRDF ingredients, as for example the core of the screened Lennard-Jones potential, we consider robust the prediction of the impurity delocalization, as well as the evolution of the mean mode energies with the number of atoms.

ACKNOWLEDGMENTS

This work has been supported in part by DGEIC (Spain), grants PB98-0124 and PB98-1247, and by the Generalitat de Catalunya Program 2000SGR-00024.

APPENDIX A:

For a spherically symmetric system the dimension of the ph space can be drastically reduced by analytically summing over the degenerate third components of the angular momentum. We illustrate this point taking as an example the Lennard-Jones contribution $V_{LJ}(\vec{r})$ to the ph interaction assuming that the ph states are coupled to yield an orbital angular momentum (L, M_L) , and a spin (S, M_S) . Using the appropriate sp quantum numbers we represent the orbital ϕ_a in coordinate and spin spaces as

$$\phi_a \equiv \phi_{a\ell_a\mu_a}(\vec{r})\chi_{\frac{1}{2}\sigma_a} \quad . \quad (\text{A1})$$

The matrix elements of the residual interaction (16) between the ph states can then be obtained as

$$\begin{aligned}
\langle mj|V_{ph}|ni\rangle = & \sum_{\sigma's} (-1)^{\frac{1}{2}-\sigma_i+\frac{1}{2}-\sigma_j} \left(\frac{1}{2}\frac{1}{2}\sigma_m - \sigma_i|SM_S\right) \left(\frac{1}{2}\frac{1}{2}\sigma_n - \sigma_j|SM_S\right) \langle\chi_{\sigma_m}|\chi_{\sigma_i}\rangle \langle\chi_{\sigma_j}|\chi_{\sigma_n}\rangle \times \\
& \sum_{\mu's} (-1)^{\ell_i-\mu_i+\ell_j-\mu_j} (\ell_m\ell_i\mu_m - \mu_i|LM_L) (\ell_n\ell_j\mu_n - \mu_j|LM_L) \times \\
& \langle\phi_{m\ell_m\mu_m}\phi_{j\ell_j\mu_j}|V_{ph}(\vec{r}_{12})|\phi_{n\ell_n\mu_n}\phi_{i\ell_i\mu_i}\rangle .
\end{aligned} \tag{A2}$$

Due to the spherical symmetry of the mean field, the sp wave functions separate in radial and angular components:

$$\phi_{a\ell\mu}(\vec{r}) = \frac{u_{a\ell}(r)}{r} Y_{\ell\mu}(\hat{r}) , \tag{A3}$$

and one can perform a multipole expansion of the ph interaction

$$V_{ph}(r_{12}) = \sum_{LM} V_L(r_1, r_2) Y_{LM}^*(\hat{r}_1) Y_{LM}(\hat{r}_2) . \tag{A4}$$

The expression for the Lennard-Jones term of Eq. (16) can be finally written in terms of the reduced matrix elements of the spherical harmonics⁵⁰ as

$$\langle mj|V_{LJ}|ni\rangle = 2\delta_{S0} \frac{1}{\sqrt{2L+1}} \langle\ell_m||Y_L||\ell_i\rangle \langle\ell_n||Y_L||\ell_j\rangle I_{mjni}^0 , \tag{A5}$$

where I_{mjni}^0 is the radial integral

$$I_{mjni}^0 = \int_0^\infty dr_1 \int_0^\infty dr_2 u_{m\ell_m}(r_1) u_{j\ell_j}(r_2) V_L(r_1, r_2) u_{n\ell_n}(r_2) u_{i\ell_i}(r_1) . \tag{A6}$$

These integrals are obtained numerically. To describe the states above the continuum threshold we have followed the usual prescription of enclosing the system in a sphere of large radius and require that the radial wave functions vanish at this distance. In this way we obtain a discrete spectrum of states that replaces the continuum. We have checked that the results are stable against reasonable changes of the radius of the sphere, which we have taken to be about 3 times larger than the mean square radius of the cluster.

- ¹ J. P. Toennies, Proceedings of the International School of Physics “Enrico Fermi”, Course CVII “*The Chemical Physics of Atomic and Molecular Clusters*” (North-Holland, Amsterdam, 1990) p. 597.
- ² K. B. Whaley, International Reviews in Phys. Chem. **13**, 41 (1994).
- ³ K. B. Whaley, Advances in Molecular Vibrations and Collision Dynamics, Vol. 3, 397 (1998).
- ⁴ J. P. Toennies and A. Vilesov, Annu. Rev. Phys. Chem. **49**, 1 (1998).
- ⁵ S. Grebenev, J. P. Toennies, and A. Vilesov, Science **279**, 2083 (1998).
- ⁶ K. Nauka and R. Miller, Phys. Rev. Lett. **82**, 4490 (1999).
- ⁷ C. Calegari et al, Phys. Rev. Lett. **83**, 5058 (1999); **84**, 1848(E) (2000).
- ⁸ Yongkyung Kwon and K. B. Whaley, Phys. Rev. Lett. **83**, 4108 (1999).
- ⁹ Ph. Sindzingre, M. L. Klein, and D. M. Ceperley, Phys. Rev. Lett. **63**, 1601 (1989).
- ¹⁰ M. V. Rama Krishna and K. B. Whaley, Phys. Rev. Lett. **64**, 1126 (1990).
- ¹¹ S. A. Chin and E. Krotschek, Phys. Rev. Lett. **65**, 2658 (1990).
- ¹² A. Belic, F. Dalfovo, S. Fantoni, and S. Stringari, Phys. Rev. B **49**, 15253 (1994).
- ¹³ Y. Kwon, D. M. Ceperley, and K. B. Whaley, J. Chem. Phys. **104**, 2341 (1996).
- ¹⁴ D. Blume, M. Lewerenz, F. Huysken, and M. Kaloudis, J. Chem. Phys. **105**, 8666 (1996).
- ¹⁵ D. Bressanini, M. Zavaglia, M. Mella, and G. Morosi, J. Chem. Phys. **112**, 717 (2000).
- ¹⁶ S. A. Chin and E. Krotschek, Phys. Rev. B **45**, 852 (1992).
- ¹⁷ S. A. Chin and E. Krotschek, Phys. Rev. B **52**, 10405 (1995).
- ¹⁸ M. Casas and S. Stringari, J. Low Temp. Phys. **79**, 135 (1990).
- ¹⁹ F. Dalfovo, Z. Phys. D **29**, 61 (1994).
- ²⁰ M. Barranco and E. S. Hernández, Phys. Rev. B **49**, 12078 (1994).
- ²¹ M. Casas, F. Dalfovo, A. Lastra, L. Serra, and S. Stringari, Z. Phys. D **35**, 67 (1995).
- ²² S. M. Gatica, E. S. Hernández, and M. Barranco, J. Chem. Phys. **107**, 927 (1997).
- ²³ F. Dalfovo, R. Mayol, M. Pi, and M. Barranco, Phys. Rev. Lett. **85**, 1028 (2000).
- ²⁴ J. Harms, M. Hartmann, J. P. Toennies, A. F. Vilesov, and B. Sartakov, J. of Mol. Spectroscopy **185**, 204 (1997).
- ²⁵ V. R. Pandharipande, S. C. Pieper, and R. B. Wiringa, Phys. Rev. B **34**, 4571 (1986).
- ²⁶ R. Guardiola and J. Navarro, Phys. Rev. Lett. **84**, 1144 (2000).
- ²⁷ R. Guardiola, Phys. Rev. B **62**, 3416 (2000).
- ²⁸ F. Castaño, M. Membrado, A. F. Pacheco, and J. Sañudo, Phys. Rev. B **48**, 12097 (1993).
- ²⁹ C. Yannouleas and U. Landman, Phys. Rev. B **54**, 7690 (1996).
- ³⁰ P. Borrmann and E. R. Hilf, Z. Phys. D **26**, S350 (1993).
- ³¹ F. Garcias, L. Serra, M. Casas, and M. Barranco, J. Chem. Phys. **108**, 9102 (1998).
- ³² M. Barranco, M. Pi, S. M. Gatica, E. S. Hernández, and J. Navarro, Phys. Rev. B **56**, 8997 (1997).
- ³³ M. Pi, R. Mayol, and M. Barranco, Phys. Rev. Lett. **82**, 3093 (1999).
- ³⁴ V. S. Babichenko and Yu. Kagan, Phys. Rev. Lett. **83**, 3458 (1999).
- ³⁵ J. Harms, J. P. Toennies, and F. Dalfovo, Phys. Rev. B **58**, 3341 (1998).
- ³⁶ J. Harms, J. P. Toennies, M. Barranco, and M. Pi, Phys. Rev. B **63**, 184513 (2000).
- ³⁷ S. Stringari and J. Treiner, J. Chem. Phys. **87**, 5021 (1987).
- ³⁸ L. Serra, J. Navarro, M. Barranco, and Nguyen Van Giai, Phys. Rev. Lett. **67**, 2311 (1991).
- ³⁹ S. Weisgerber and P.-G. Reinhard, Z. Phys. D **23**, 275 (1992).
- ⁴⁰ S. Weisgerber and P.-G. Reinhard, Ann. Physik **2**, 666 (1993).
- ⁴¹ M. Barranco, D. M. Jezek, E. S. Hernández, J. Navarro, and L. Serra, Z. Phys. D **28**, 257 (1993).
- ⁴² M. Barranco, J. Navarro, and A. Poves, Phys. Rev. Lett. **78**, 4729 (1997).
- ⁴³ M. Barranco, F. Garcias, L. Serra, and M. Casas, J. Low Temp. Phys. **113**, 381 (1998).
- ⁴⁴ Y. M. Engel, D. M. Brink, K. Goeke, S. J. Krieger, and D. Vautherin, Nucl. Phys. A **249**, 215 (1975).
- ⁴⁵ K. T. Tang and J. P. Toennies, Z. Phys. D **1**, 91 (1986).
- ⁴⁶ R. T. Pack, E. Piper, G. A. Pfeffer, and J. P. Toennies, J. Chem. Phys. **80**, 4940 (1984).
- ⁴⁷ J. P. Blaizot and G. Ripka, *Quantum theory of finite systems*, MIT Press, Cambridge, MA (1986).
- ⁴⁸ J. W. Negele and H. Orland, *Quantum many-particle systems*, Addison-Wesley, New York (1988).
- ⁴⁹ A. B. Migdal, *The theory of finite Fermi systems*, Wiley, New York (1967).
- ⁵⁰ E. U. Condon and H. Odabasi, *Atomic Structure*, Cambridge University Press, New York (1980).
- ⁵¹ S. Stringari, Phys. Lett. A **107**, 36 (1985).
- ⁵² J. Dupont-Roc, M. Himbert, N. Pavloff, and J. Treiner, J. Low Temp. Phys. **81**, 31 (1990).
- ⁵³ C. García-Recio, J. Navarro, Nguyen Van Giai, and L. L. Salcedo, Ann. Phys. (N.Y.) **214**, 293 (1992).

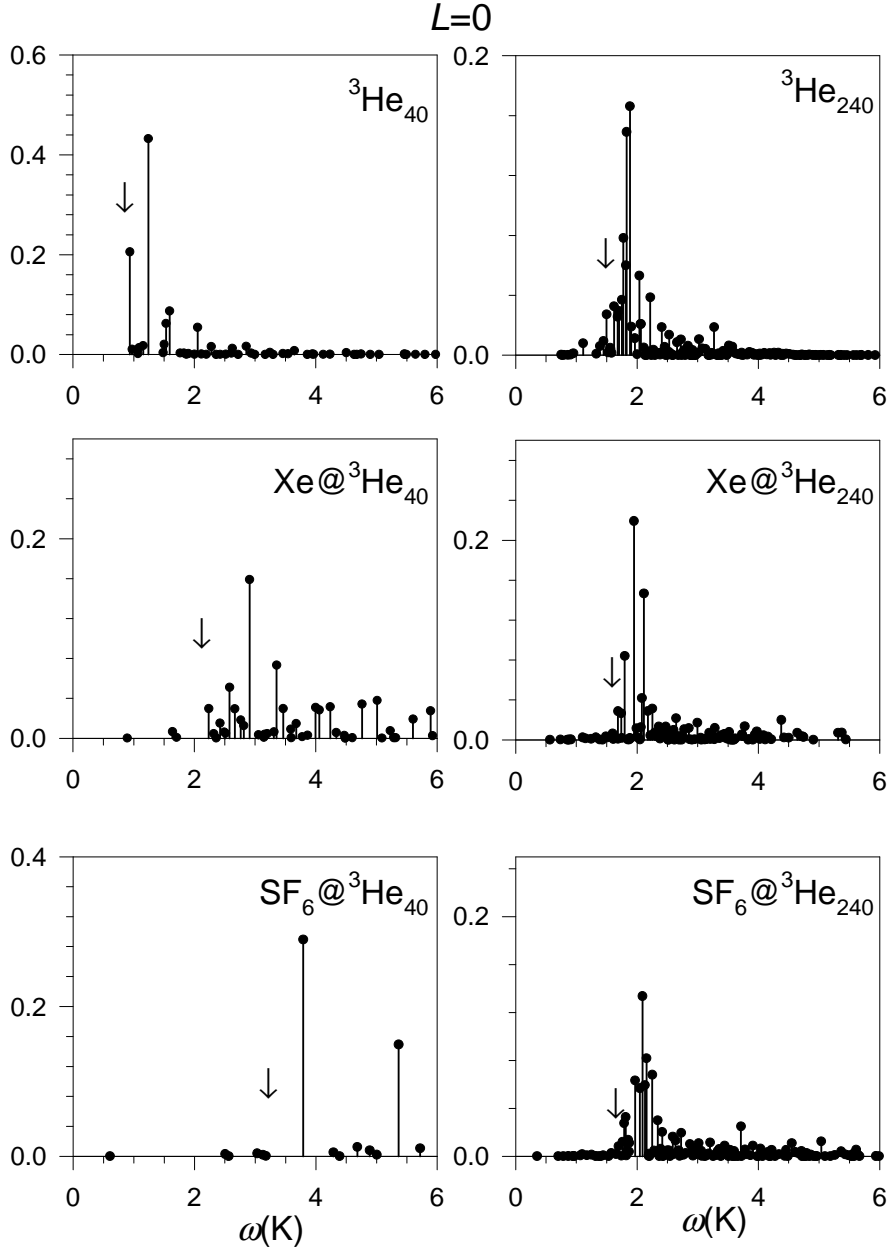


Fig.1

FIG. 1. Comparison between the monopole spectrum of pure and doped drops. Each excited state is represented by a vertical stick whose height gives its fractional contribution to the energy weighted sum rule. The arrows indicate the position of the atom emission threshold in each case.

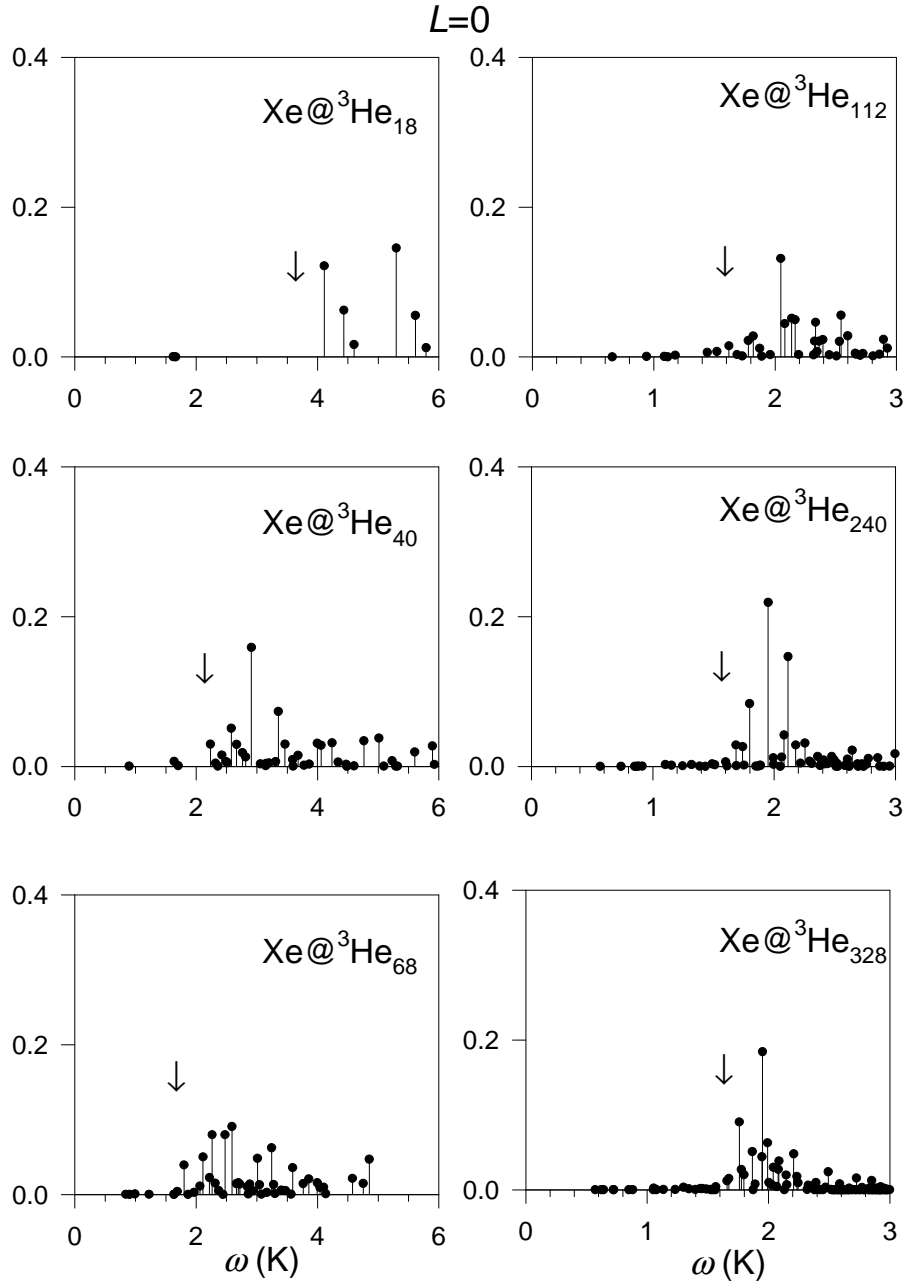


Fig.2

FIG. 2. Same as Fig. 1 for the monopole spectrum of drops doped with Xe.

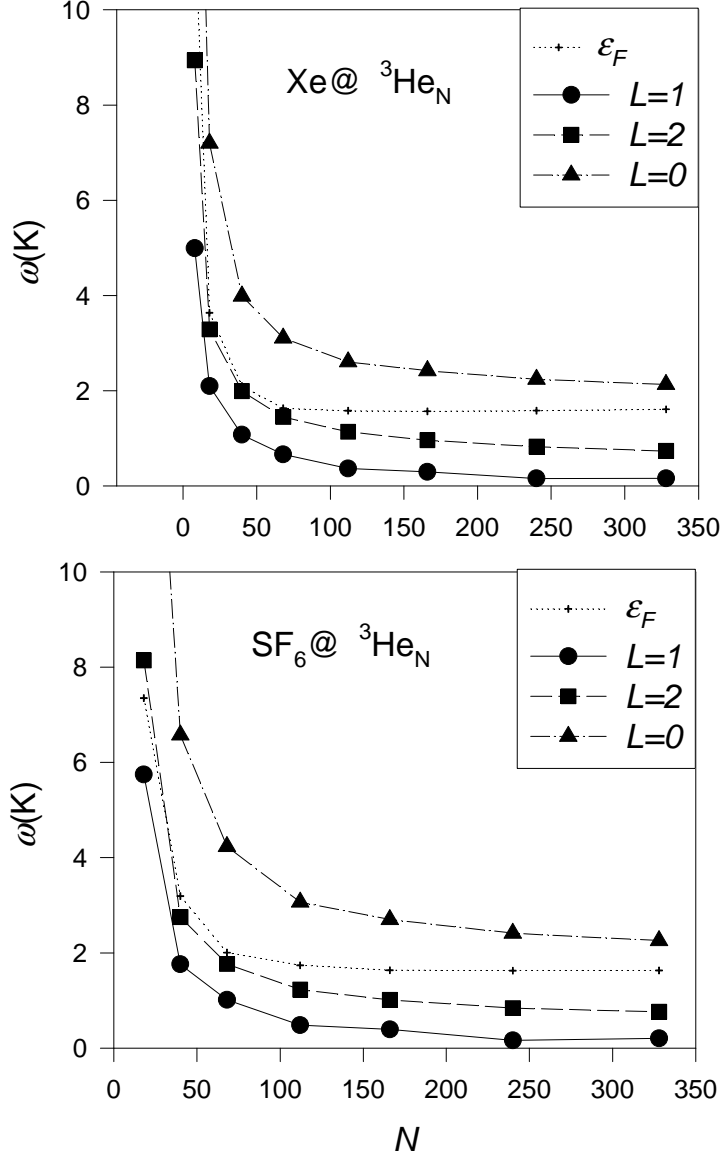


Fig.3

FIG. 3. Mean excitation energies $\bar{\omega}$ (K) and chemical potential changed of sign ε_F as a function of N for $^3\text{He}_N$ drops doped with Xe and SF_6 . The lines have been drawn to guide the eye.

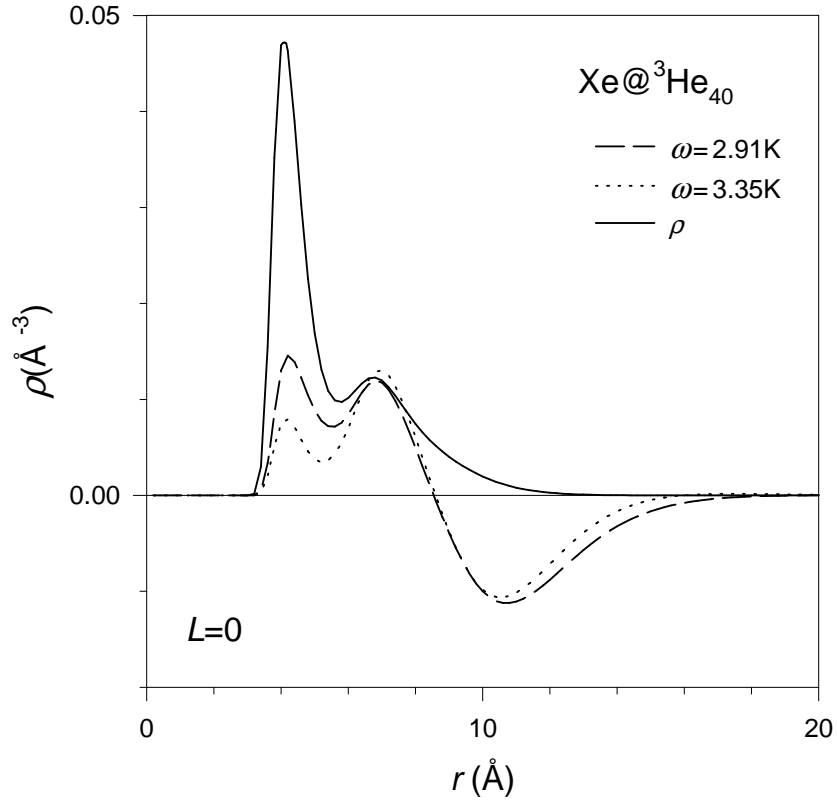


Fig.4

FIG. 4. Transition densities (arbitrary scale) corresponding to the more intense monopole states of $\text{Xe}+^3\text{He}_{40}$. The ground state density $\rho(r)$ is also shown. The transition densities have been scaled to have a common value at $r = 10 \text{ \AA}$.

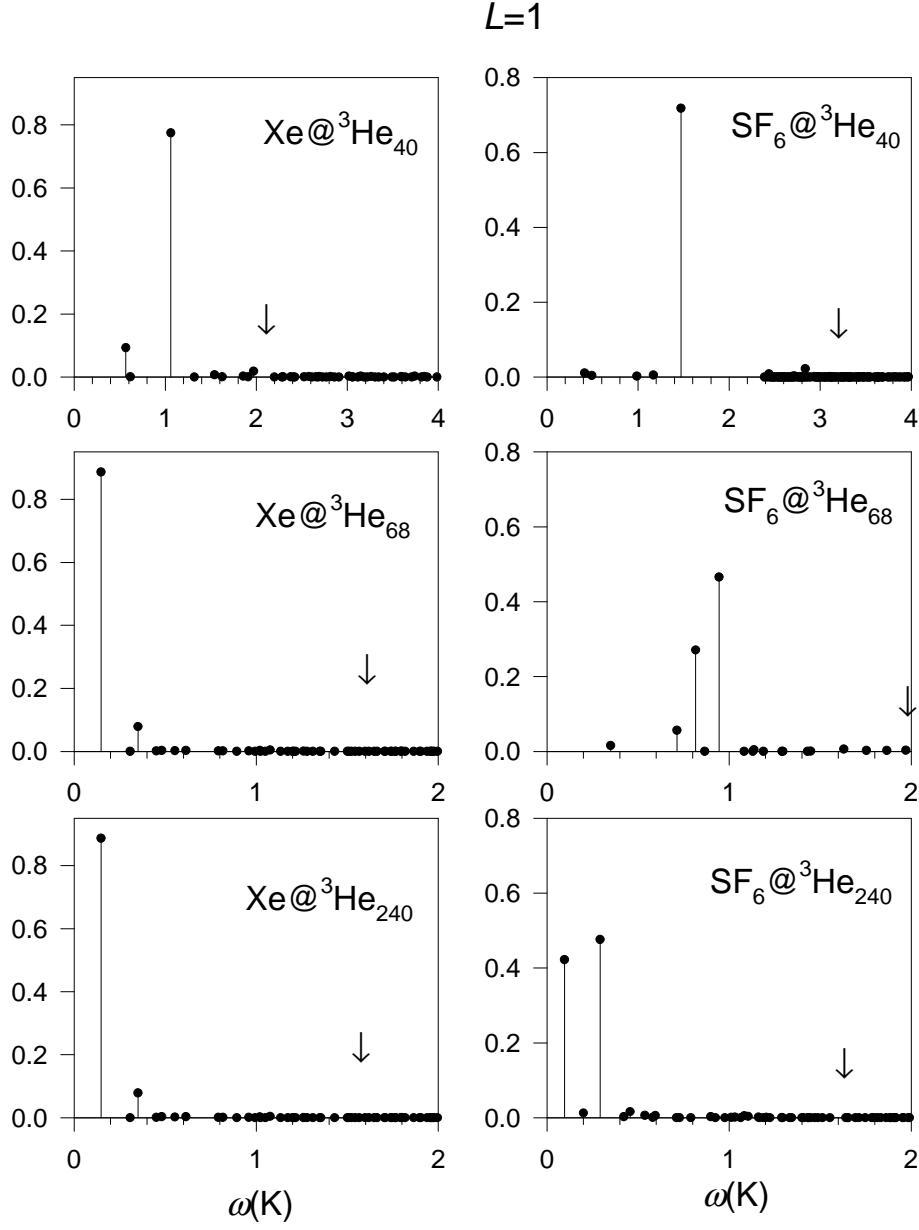


Fig.5

FIG. 5. Same as Fig. 1 for the dipole spectrum of doped drops.

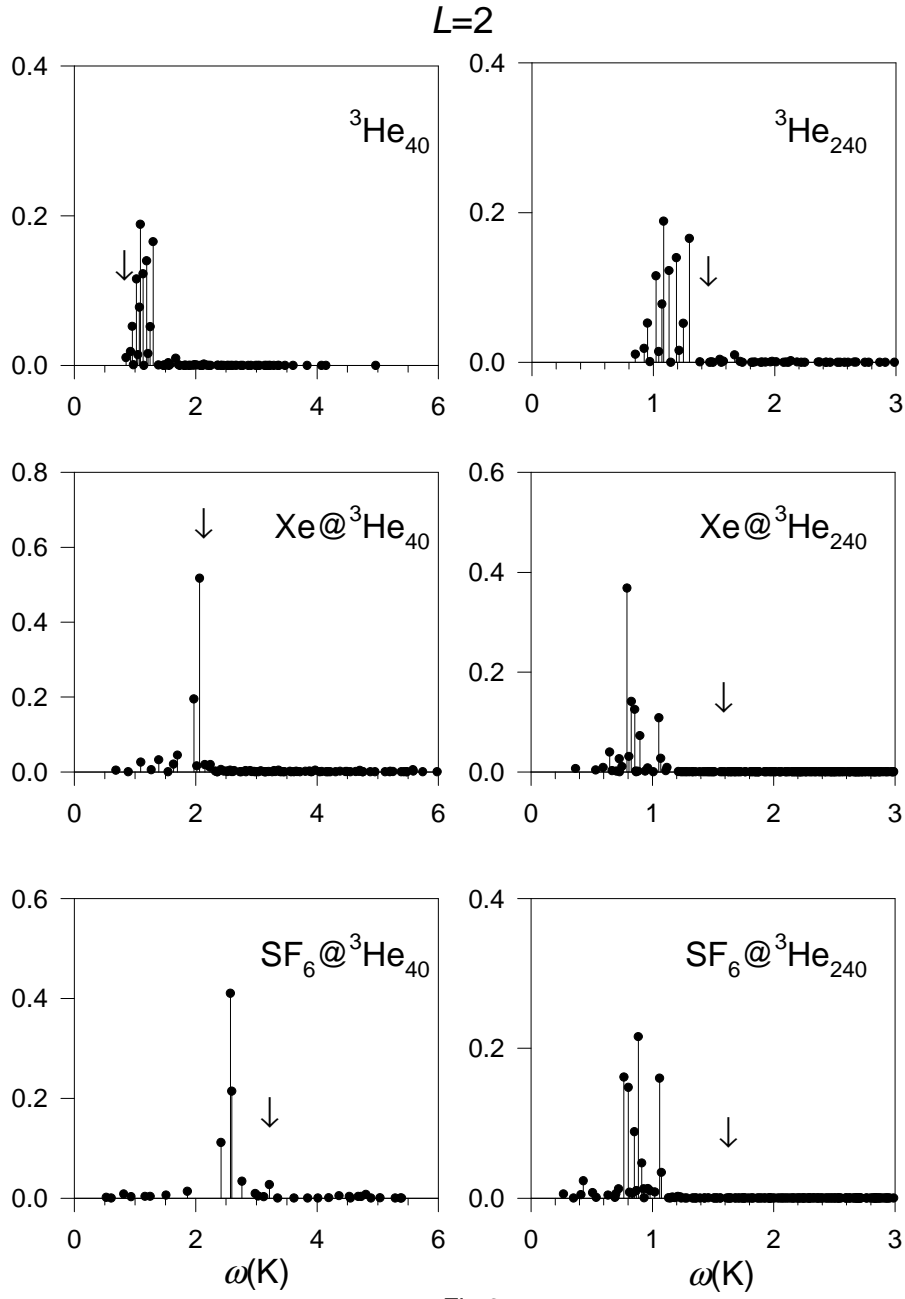


Fig.6

FIG. 6. Same as Fig. 1. for the quadrupole spectrum.

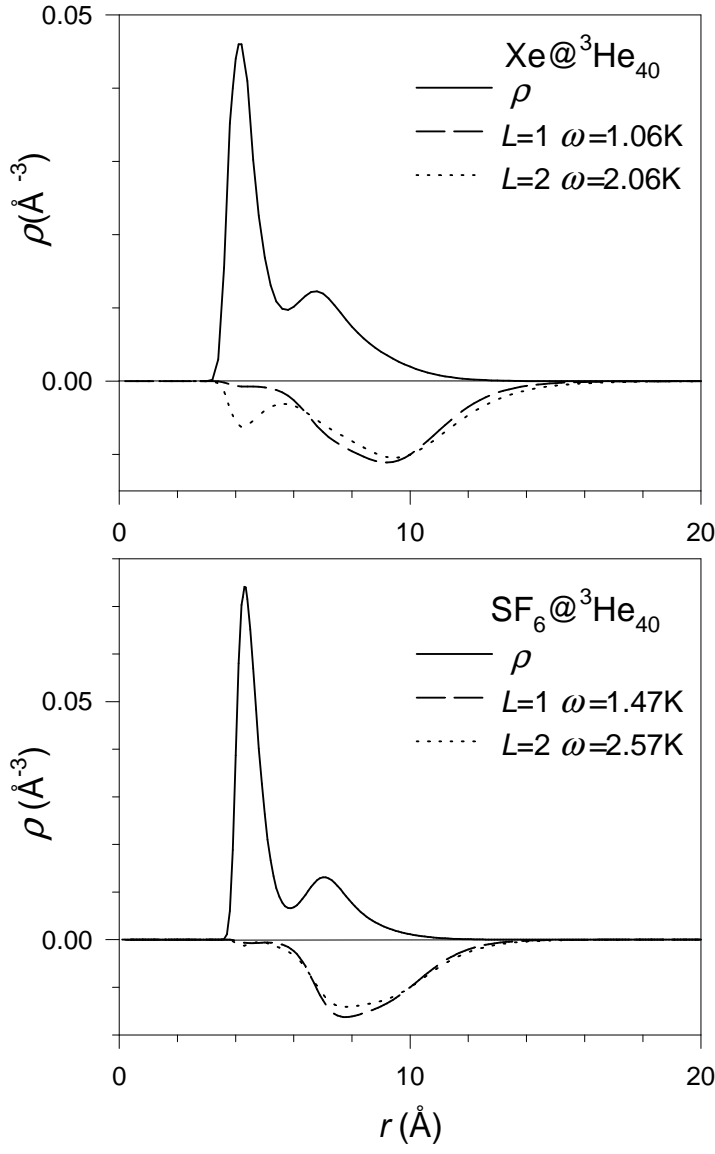


Fig.7

FIG. 7. Transition densities (arbitrary scale) corresponding to the more intense $L = 1$ and 2 peaks and ground state density $\rho(r)$ of the ${}^3\text{He}_{40}$ drop doped with Xe and SF_6 . Scaling factors as in Fig. 4 have been used.